Anomalous Cooling and Overcooling of Active Colloids

Fabian Jan Schwarzendahl* and Hartmut Löwen
Institut für Theoretische Physik II: Weiche Materie, Heinrich-Heine-Universität Düsseldorf, 40225 Düsseldorf, Germany

(Received 10 November 2021; revised 14 July 2022; accepted 10 August 2022; published 23 September 2022)

The phenomenon that a system at a hot temperature cools faster than at a warm temperature, referred to as the Mpemba effect, has recently been realized for trapped colloids. Here, we investigate the cooling and heating process of a self-propelled active colloid using numerical simulations and theoretical calculations with a model that can be directly tested in experiments. Upon cooling, activity induces a Mpemba effect and the active particle transiently escapes an effective temperature description. At the end of the cooling process the notion of temperature is recovered and the system can exhibit even smaller temperatures than its final temperature, a surprising phenomenon which we refer to as activity-induced overcooling.

DOI: 10.1103/PhysRevLett.129.138002

When water is cooled down to be frozen, it seems intuitive that the cooler the water, the faster it will freeze. Contrary to that, about 2300 years ago, Aristotle already noticed that "to cool hot water quickly, begin by putting it in the sun" [1], observing that hot water can be cooled and also frozen faster than warm water. The first systematic study to investigate this effect was conducted in the 1960s by Mpemba [2]. Thereafter, numerous experimental studies followed, but no consensus on the cause of the "Mpemba effect" for water was found, so far [3–8]. Recently, the Mpemba effect was discovered for colloidal particles that are subjected to a thermal quench [9], where the colloids were confined to a double well potential, mimicking the liquid and frozen state of water. The experimental findings match theoretical predictions giving a clear explanation of the underlying effect [10,11] and provide an experimental road to recent theoretical advances in understanding principles of the Mpemba effect [12–17].

Active colloids that are self-propelling, constantly pump energy into the system and, therefore, are inherently out of equilibrium [18]. Active colloidal particles have been realized in various experimental systems [18] and can show fascinating effects such as wall accumulation [19–21], activity induced ratchet motion [22,23], motility induced phase separation [24,25], or vortex formation [26]. Here, we investigate the cooling and heating process of trapped active colloids and find that they exhibit, not only a Mpemba effect, but also overcooling, i.e., they transiently reach a temperature that is lower than its final steady state temperature [Fig. 1(d)]. However, before overcooling happens, the system deviates significantly from any reference system at a prescribed temperature, i.e., it escapes an effective temperature description [Fig. 1(d)]. Irrespective of the validity of the effective temperature concept during relaxation, the active colloids can show a Mpemba effect.

To illustrate the Mpemba effect, imagine two systems, one of which is at an initial warm temperature, and the second is at an initial hot temperature. Both systems are then cooled down to an imposed cold temperature [Fig. 1(a)]. Normally, the warm system cools faster than the hot system and a Mpemba effect occurs if the hot system

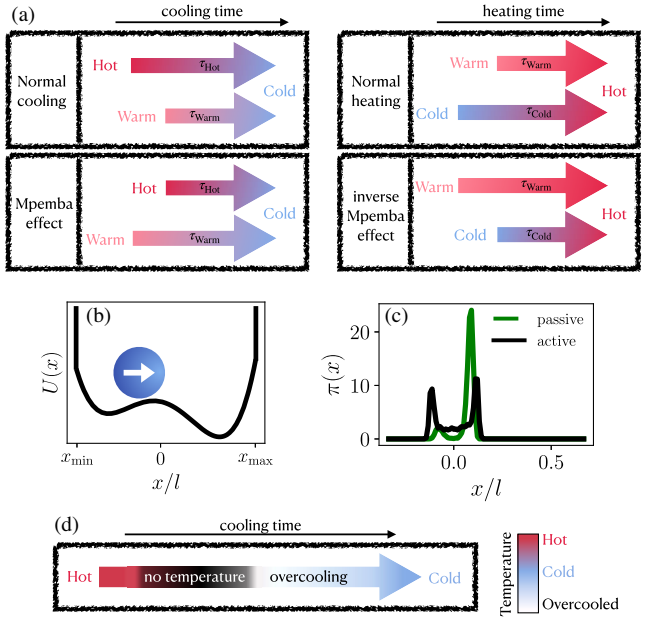

FIG. 1. (a) Cooling and heating scenarios, where each colored arrow represents a cooling or heating process. The arrows' length displays the time that the system needs to cool down (left) or heat up (right). (b) Asymmetric potential with walls $U(x)$ as a function of space that the active colloid (blue circle) is subjected to. (c) Occupation probability $\pi(x)$ of an active (black line) and passive (green line) colloid in the external potential shown in (b). (d) An overcooling scenario, where during the cooling process the system escapes an effective temperature description (black represents the regime without a temperature definition) and then goes to lower temperatures than the final temperature. The color code of the arrow represents the temperature.

cools faster than the warm one. Analogously, a cold system can heat up faster than the warm one [Fig. 1(a)], which is referred to as the inverse Mpemba effect [12,27]. The Mpemba effect for a passive colloid [9] in an asymmetric potential [similar to Fig. 1(b)] can be understood as follows: a hot particle cooling down has enough residual energy to overcome the barrier and, subsequently, quickly relaxes to the cold state. On the other hand, a warm particle, having effectively less residual energy, will take a longer time overcoming the potential barrier.

We investigate the cooling and heating process of active colloids in a confining asymmetric potential [Fig. 1(b)]. An active Brownian particle subjected to fluctuations with a temperature T and performing overdamped motion is modeled in one spatial dimension by the following equation:

$$\frac{dx}{dt} = v_0 n - \frac{1}{\gamma}\partial_x U(x) + \eta(t), \tag{1}$$

where v_0 is the self-propulsion speed, and n is the direction of propulsion. The propulsion direction is inverted after a time t_p, which is drawn from a normalized exponential distribution $p(t_p) = 1/\tau_p e^{-t_p/\tau_p}$ with a characteristic persistence time τ_p. Furthermore, $\eta(t)$ is a Gaussian white noise with zero mean and variance $\langle \eta(t)\eta(t')\rangle = 2D_T\delta(t-t')$, where the noise strength can be identified with the particles translational diffusion constant D_T. The latter is controlled by the temperature T, as $D_T = (k_B T/\gamma)$, where k_B is the Boltzmann constant, and γ is the friction coefficient. The particle is exposed to an external double well potential

$$U(x) = \begin{cases} -F_0 x, & \text{if } x < x_{\min}, \\ F_B[(1-x^2)^2 - \frac{1}{2}x], & \text{if } x_{\min} < x < x_{\max}, \\ F_0 x, & \text{if } x > x_{\max}. \end{cases} \tag{2}$$

This potential is displayed in Fig. 1(b), where the terms in Eq. (2), proportional to F_0, represent repulsive walls at positions $x_{\min}$ and $x_{\max}$, and the term proportional to F_B models an asymmetric potential with two minima of different height. The size of the box confining the particle, $l = |x_{\max} - x_{\min}|$, provides a natural unit of length, and combined with the translational diffusion constant, there is a natural unit of time $\tau_D = l^2/D_T$ and velocity $v_D = l/\tau_D$. The system described by Eq. (1) can be realized using a Janus colloid [18,28], yielding a self-propulsion together with optical [9,29] or acoustic [30] traps that establish an external potential and a half channel that confines the motion of the colloid into one spatial dimension [31,32] (see the Supplemental Material [33] for a sketch) [34–41].

In the following, we generate the probability distribution $P(x,t)$ to find the particle at position x and time t from Eq. (1). Typical steady state distributions denoted by $\pi(x)$ for a passive ($v_0 = 0$) and an active particle ($v_0 \neq 0$) are shown in Fig. 1(c), where the particles are localized around the two minima of the external potential. Additionally, the distribution of the active particle is enhanced toward the wall regions due to the wall accumulation effect that arises from the persistence and active motion of the particle [42–52].

Now, consider two systems which are initially in their steady state at a hot T_{hot} (hot particle) and warm temperature T_{warm} (warm particle) with $T_{\text{hot}} > T_{\text{warm}}$ [Fig. 2(a)].

Figures 2(a)–2(c) reveal how the distributions of the warm and hot particles relax and finally reach their new steady state distributions $\pi_{\text{cold}}(x)$ after an instantaneous thermal quench to T_{cold} [Fig. 2(c)]. The hot particle relaxes faster [Fig. 2(b)] than the warm particle [Fig. 2(c)], which is an anomalous cooling referred to as the Mpemba effect. The intuitive underlying reason for the Mpemba effect is related to the fact that the distribution of the warm particle is localized into the minima of the external potential [Eq. (2)], such that the particle needs to hop over the potential barrier to relax to the cold distribution. On the other hand, the distribution of the hot particle is not

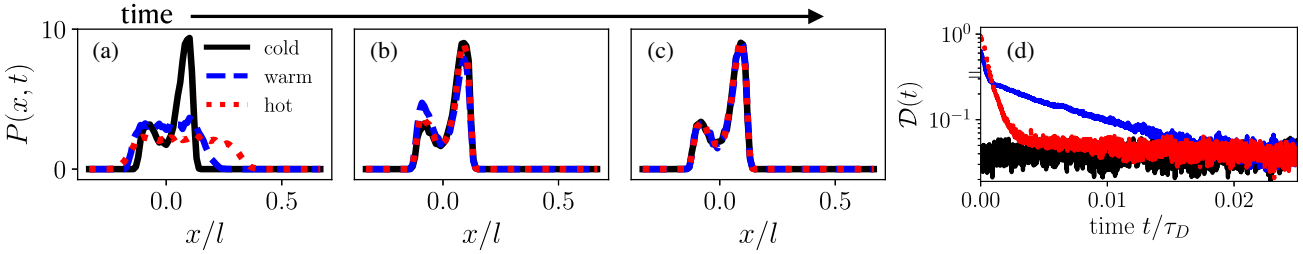

FIG. 2. (a)–(c) Probability distributions of active colloids. A hot (red dotted line, $T_{\text{hot}} = 2500T_{\text{cold}}$), a warm (blue dashed line, $T_{\text{warm}} = 50T_{\text{cold}}$), and cold (black solid line) colloid is shown. (a) Initial steady state distributions at $t = 0$. A temperature quench is applied at this time. (b) Distributions at $t = 3 \times 10^{-3}\tau_D$. The hot colloid has relaxed close to T_{cold}. (c) Distributions at $t = 50 \times 10^{-3}\tau_D$. The warm colloid has also relaxed close to T_{cold}. (d) Relaxation dynamics of the "distance" $\mathcal{D}(t)$ measured by the partitioning between probability distributions and the steady state distribution of a cold colloid for an initially hot, warm, and cold colloid. [Parameters: $F_0/(\gamma v_D) = 1.5 \times 10^5$, $F_B/(\gamma v_D) = 24$, $x_{\min}/l = -1/3$, $x_{\max}/l = 2/3$, $v_0/v_D = 120$, $\tau_p/\tau_D = 2 \times 10^{-4}$.].

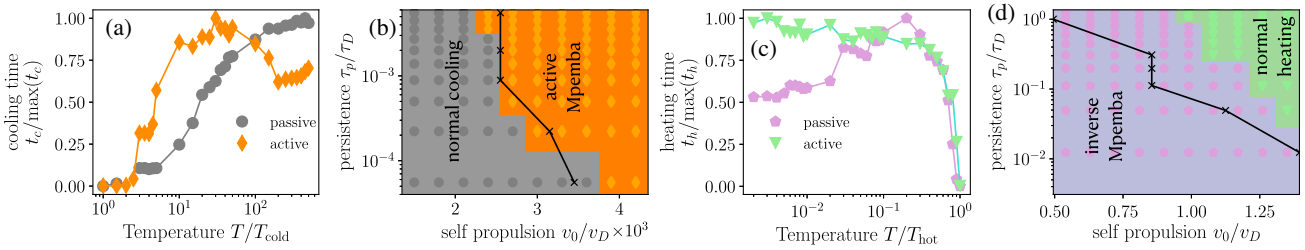

FIG. 3. (a) Cooling time as a function of initial temperature T to final temperature $T_{\rm cold}$ for passive (gray circles) and active (orange diamonds, $v_0/v_D = 3.9\times10^3$, $\tau_p/\tau_D = 5\times10^{-4}$) particles. (b) Cooling state diagram as a function of self-propulsion and persistence showing normal cooling and the active Mpemba effect, where the black crosses show theoretical transition points. [Parameters (a)-(b): $F_0/(\gamma v_D) = 1.5\times10^5$, $F_B/(\gamma v_D) = 24$, $x_{\rm min}/l = -1/2$, $x_{\rm max}/l = 1/2$.] (c) Heating time as a function of initial temperatures T to final temperature $T_{\rm hot}$ for active (green triangles, $v_0/v_D = 9$, $\tau_p/\tau_D = 1.2$) and passive (purple pentagons) particles. (d) Heating state diagram for varying self-propulsion and persistence, where the black crosses show theoretical transition points. [Parameters (c)–(d): $F_0/(\gamma v_D) = 450$, $F_B/(\gamma v_D) = 0.054$, $x_{\rm min}/l = -2/9$, $x_{\rm max}/l = 7/9$.].

localized and almost no hopping processes are required in order to relax. Since the hopping processes over the barrier take a long time, the warm particle will relax slower than the hot particle.

To get further insight into the relaxation process, the distance between the cooled steady state distribution $\pi_{\rm cold}(x)$ and the probability distribution $P(x,t)$ of a particle during the cooling process is quantified. In order to construct such an abstract distance measure, the spatial components of both $\pi_{\rm cold}(x)$ and $P(x,t)$ are discretized into N grid points, giving $\pi_{i,\rm cold}$ and $P_i(t)$, respectively, resulting in the following distance measure:

$$\mathcal{D}(t) = \frac{1}{N}\sum_{i=0}^{N} |P_i(t) - \pi_{i,\rm cold}|. \tag{3}$$

Figure 2(d) shows the distance measure Eq. (3), which quantifies the cooling process of the hot and warm particles. From this measure, a cooling time t_c can be extracted, defined as the time at which $\mathcal{D}(t)$ has decayed to zero, or, here, to the noise level.

Exploring a range of initial temperatures T yields the cooling curves shown in Fig. 3(a). For active particles ($v_0 \neq 0$), the cooling curve is nonmonotonic, giving rise to a Mpemba effect that is induced by activity. Here, activity changes the probability distributions of the particles by inducing a wall accumulation [Fig. 1(c)], which, in turn, enables the Mpemba effect. For the parameters chosen, passive particles ($v_0 = 0$) show normal cooling [Fig. 3(a)], that is, the cooling time increases monotonically with initial temperature. Figure 3(b) shows the dependence of the active Mpemba effect on the self-propulsion and persistence of the particle, see the Supplemental Material [33] for details. For low persistence and self propulsion, there is no Mpemba effect for our choice of parameters, while at higher self-propulsion and persistence, activity induces a Mpemba effect.

A statistically equivalent version of Eq. (1) in terms of a probability $P(x,t)$ to find the particle at position x and time t and its polarization $P^*(x,t)$ is given by the Smoluchowski equation

$$\partial_t P = -v_0\partial_x P^* + \frac{1}{\gamma}\partial_x\{[\partial_x U(x)]P\} + D_T\partial_x^2 P, \tag{4}$$

$$\partial_t P^* = -v_0\partial_x P + \frac{1}{\gamma}\partial_x\{[\partial_x U(x)]P^*\} + D_T\partial_x^2 P^* - \frac{2}{\tau_p}P^*, \tag{5}$$

which is solved using an eigenfunction expansion (see the Supplemental Material [33]). The resulting cooling curves agree with the numerical approach using Eq. (1) (see the Supplemental Material [33]) and the transition line (black line) from normal cooling to active Mpemba effect is shown in Fig. 3(b). The dependence of the Mpemba effect on the compartment size and persistence length is discussed in the Supplemental Material [33].

Recently, the inverse Mpemba effect, where a cold particle heats faster than a warm one, has been discovered for passive colloids [27]. Figure 3(c) shows the heating curves of passive and active particles toward the temperature $T_{\rm hot}$. Here, a passive particle has a nonmonotonic heating curve, an inverse Mpemba effect [27], which is eliminated by the active motion [see, also, Fig. 3(d)].

An effective temperature is defined based on the distance measure $\mathcal{D}(t)$ that can be traced in time. At a given time t the probability distribution $P(x,t)$ is compared to all possible steady states $\pi_{T_{\rm eff}}(x)$ with effective temperatures $T_{\rm eff}$, explicitly

$$\mathcal{D}_{T_{\rm eff}}(t) = \sum_i |P_i(t) - \pi_{i,T_{\rm eff}}|, \tag{6}$$

which is discretized as before. The temperature $T_{\rm eff}$ for which $\mathcal{D}_{T_{\rm eff}}(t)$ is minimal, is then defined as the effective

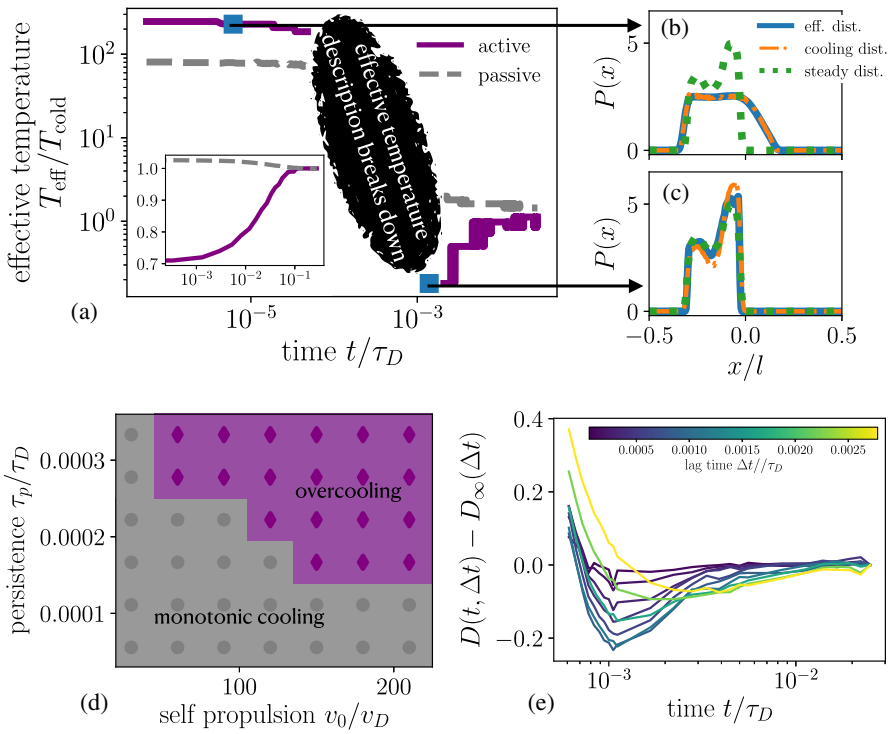

FIG. 4. (a) Effective temperature $T_{\rm eff}$ as a function of time for an active (purple solid line, $v_0/v_D = 150$, $\tau_p/\tau_D = 2.7 \times 10^{-4}$) and passive (grey dashed line) particle. The initial temperature corresponds to the hot particle in Fig. 2. At intermediate times, the effective temperature description breaks down. Inset: Effective temperature $T_{\rm eff}$ as a function of time extracted from our theoretical approach [Inset parameters: $F_B/(\gamma v_D) = 4.4$, $x_{\rm min}/l = -0.36$, $x_{\rm max}/l = 0.63$, $v_0/v_D = 27.5$, $\tau_p/\tau_D = 1.6 \times 10^{-3}$]. (b)–(c) Probability distributions after time t of the cooling process (orange dash-dotted line), effective distribution $\pi_{T_{\rm eff}}$ (solid blue line) and final steady state (green dotted line). (b) shows a typical state at the beginning of the cooling process and (c) a state where the system is overcooled. (d) State diagram showing overcooling (purple diamonds) and monotonic cooling (grey circles) for varying self-propulsion and persistence. (e) Reduced lag diffusion as a function of time for different lag times (color code, $v_0/v_D = 150$, $\tau_p/\tau_D = 2.7 \times 10^{-4}$). [Parameters: $F_0/(\gamma v_D) = 1.5 \times 10^5$, $F_B/(\gamma v_D) = 15$, $x_{\rm min}/l = -1/3$, $x_{\rm max}/l = 2/3$.].

temperature of the system. When cooling down to $T_{\rm cold}$, the effective temperature of a passive system decays monotonically, until it reaches its steady state [Fig. 4(a)]. Turning on activity, the particles probability distribution quickly enters a regime where it is not captured by a steady state distribution. Hence, the effective temperature description breaks down. This is quantified by the distance measure, which has to be sufficiently small to define a temperature, here, $\mathcal{D}_{T_{\rm eff}}(t) < 0.1$ is used (see, also, the Supplemental Material [33]). Even if no effective temperature can be assigned to the active colloid at time t, $\mathcal{D}_{T_{\rm eff}}(t)$ can still show how far the instantaneous distribution is from the final, steady-state cold distribution. In this sense, irrespective of the validity of the effective temperature concept during relaxation, Fig. 2(d) does show a Mpemba-type effect: the initially hot active colloid does, indeed, approach the cold state faster than the initially warm colloid. However, toward the end of the cooling process, the effective temperature description is recovered and takes values that are lower than the final steady state temperature [Fig. 4(a)]. This surprising effect is an activity induced overcooling of the system. The probability distributions [Fig. 4(c)] show how the distribution $P(x,t)$ is closer to an effective distribution $\pi_{T_{\rm eff}}(x)$ than to the distribution of the cold state $\pi_{\rm cold}$, meaning that the particle has an effective temperature $T_{\rm eff} < T_{\rm cold}$. The theoretical approach using Eqs. (4) and (5) also shows an overcooling [Fig. 4(a), (inset)], where the probability distribution was numerically evaluated in the long time limit, which was used to find the effective temperature with Eq. (6). Intuitively, overcooling is related to the particle hopping over the potential barrier to achieve the correct partitioning needed in the final steady state. The barrier separates two regions, and if the probability to find the particle in the right region is higher than required for the final steady state, the particle needs to hop over the barrier. Hopping processes are typically slow and, therefore, will dominate the final relaxation. During this relaxation the absolute peak height is higher than needed for the final steady state, which corresponds to a lower effective temperature just before final relaxation. Activity helps to achieve this imbalance of occupancy, since it enhances the probability of finding the particle at the wall,

enabling a strong peak in the right region. This overcooling mechanism is qualitatively different than that found for a mean-field Ising model [13].

Figure 4(d) displays the dependence of the overcooling effect on the active motion of the particle. At low self-propulsion and persistence, monotonic cooling is recovered, while increasing both leads to an overcooling.

Our choice for an effective temperature is not unique, and we computed the effective temperature using several other definitions (see the Supplemental Material [33]), which display the same overcooling effect. Here, as an alternative measure for the effective temperature [53], the lag diffusion defined as $D(t,\Delta t) = (1/N_r)\sum_i^{N_r}[x_i(t+\Delta t) - x_i(t)]^2/\Delta t$ is computed, where t is the time at which we start measuring the diffusion and Δt is the lag time. N_r is the number of realizations of trajectories $x_i(t)$ that are simulated. By computing the reduced lag diffusion $D(t,\Delta t) - D_\infty(\Delta t)$, where $D_\infty(\Delta t)$ is the diffusion at the end of our simulations, it is observed that the diffusion shows lower values than its final steady state value [Fig. 4(e)], which is an overcooling of the system. This effect is purely induced by activity, it is not present for the corresponding passive system (see the Supplemental Material [33]).

We have investigated the interplay of two nonequilibrium phenomena, the cooling or heating process of a colloid, and its active motion, showing that the active motion of a particle can fundamentally change the relaxation process. In principle, our model allows for a direct experimental verification with active colloids. In the future, it will be interesting to see how this translates to higher dimensions, and many particle systems. Overcooling enables a refrigerator to transiently cool a system to lower temperatures than the prescribed temperature, which raises the question how the effect optimizes the function of heat engines [54,55]. While we focused on active colloids in this Letter, similar effects might arise for biological microswimmers, such as bacteria or microalgae, which can change their motility pattern and, therefore, their effective temperature in response due to external stimulus [56].

We thank Lorenzo Caprini for insightful discussions and Theresa Schwarzendahl for proof reading the manuscript. H. L. was supported within the SPP 2065 (Project No. LO 418/25-1).

*Fabian.Schwarzendahl@hhu.de

[1] Aristotle, *Meteorology Book 1, Part 12* (The Clarendon Press, Oxford, 1923), (translated by E. W. Webster).
[2] E. B. Mpemba and D. G. Osborne, Cool?, Phys. Educ. **4**, 172 (1969).
[3] M. Jeng, The Mpemba effect: When can hot water freeze faster than cold?, Am. J. Phys. **74**, 514 (2006).
[4] B. Wojciechowski, I. Owczarek, and G. Bednarz, Freezing of aqueous solutions containing gases, Cryst. Res. Technol. **23**, 843 (1988).
[5] D. Auerbach, Supercooling and the Mpemba effect: When hot water freezes quicker than cold, Am. J. Phys. **63**, 882 (1995).
[6] M. Vynnycky and N. Maeno, Axisymmetric natural convection-driven evaporation of hot water and the Mpemba effect, Int. J. Heat Mass Transfer **55**, 7297 (2012).
[7] M. Vynnycky and S. Kimura, Can natural convection alone explain the Mpemba effect?, Int. J. Heat Mass Transfer **80**, 243 (2015).
[8] H. C. Burridge and P. F. Linden, Questioning the Mpemba effect: Hot water does not cool more quickly than cold, Sci. Rep. **6**, 37665 (2016).
[9] A. Kumar and J. Bechhoefer, Exponentially faster cooling in a colloidal system, Nature (London) **584**, 64 (2020).
[10] J. Bechhoefer, A. Kumar, and R. Chétrite, A fresh understanding of the Mpemba effect, Nat. Rev. Phys. **3**, 534 (2021).
[11] R. Chétrite, A. Kumar, and J. Bechhoefer, The metastable Mpemba effect corresponds to a non-monotonic temperature dependence of extractable work, Front. Phys. **9**, 141 (2021).
[12] Z. Lu and O. Raz, Nonequilibrium thermodynamics of the Markovian Mpemba effect and its inverse, Proc. Natl. Acad. Sci. U.S.A. **114**, 5083 (2017).
[13] I. Klich, O. Raz, O. Hirschberg, and M. Vucelja, Mpemba Index and Anomalous Relaxation, Phys. Rev. X **9**, 021060 (2019).
[14] A. Gal and O. Raz, Precooling Strategy Allows Exponentially Faster Heating, Phys. Rev. Lett. **124**, 060602 (2020).
[15] F. Carollo, A. Lasanta, and I. Lesanovsky, Exponentially Accelerated Approach to Stationarity in Markovian Open Quantum Systems through the Mpemba Effect, Phys. Rev. Lett. **127**, 060401 (2021).
[16] N. Vadakkayil and S. K. Das, Should a hotter paramagnet transform quicker to a ferromagnet? Monte Carlo simulation results for Ising model, Phys. Chem. Chem. Phys. **23**, 11186 (2021).
[17] A. Megías, A. Santos, and A. Prados, Thermal versus entropic Mpemba effect in molecular gases with nonlinear drag, Phys. Rev. E **105**, 054140 (2022).
[18] C. Bechinger, R. Di Leonardo, H. Löwen, C. Reichhardt, G. Volpe, and G. Volpe, Active particles in complex and crowded environments, Rev. Mod. Phys. **88**, 045006 (2016).
[19] N. Narinder, J. R. Gomez-Solano, and C. Bechinger, Active particles in geometrically confined viscoelastic fluids, New J. Phys. **21**, 093058 (2019).
[20] G. Volpe, I. Buttinoni, D. Vogt, H.-J. Kümmerer, and C. Bechinger, Microswimmers in patterned environments, Soft Matter **7**, 8810 (2011).
[21] C. Maggi, J. Simmchen, F. Saglimbeni, J. Katuri, M. Dipalo, F. De Angelis, S. Sanchez, and R. Di Leonardo, Self-assembly of micromachining systems powered by Janus micromotors, Small **12**, 446 (2016).
[22] R. Di Leonardo, L. Angelani, D. Dell'Arciprete, G. Ruocco, V. Iebba, S. Schippa, M. P. Conte, F. Mecarini, F. De Angelis, and E. Di Fabrizio, Bacterial ratchet motors, Proc. Natl. Acad. Sci. U.S.A. **107**, 9541 (2010).

[23] J. Rodenburg, S. Paliwal, M. De Jager, P. G. Bolhuis, M. Dijkstra, and R. Van Roij, Ratchet-induced variations in bulk states of an active ideal gas, J. Chem. Phys. **149**, 174910 (2018).
[24] I. Buttinoni, J. Bialké, F. Kümmel, H. Löwen, C. Bechinger, and T. Speck, Dynamical Clustering and Phase Separation in Suspensions of Self-Propelled Colloidal Particles, Phys. Rev. Lett. **110**, 238301 (2013).
[25] J. Palacci, S. Sacanna, A. P. Steinberg, D. J. Pine, and P. M. Chaikin, Living crystals of light-activated colloidal surfers, Science **339**, 936 (2013).
[26] A. Bricard, J.-B. Caussin, D. Das, C. Savoie, V. Chikkadi, K. Shitara, O. Chepizhko, F. Peruani, D. Saintillan, and D. Bartolo, Emergent vortices in populations of colloidal rollers, Nat. Commun. **6**, 7470 (2015).
[27] A. Kumar, R. Chétrite, and J. Bechhoefer, Anomalous heating in a colloidal system, Proc. Natl. Acad. Sci. U.S.A. **119**, e2118484119 (2022).
[28] J. R. Gomez-Solano, S. Samin, C. Lozano, P. Ruedas-Batuecas, R. van Roij, and C. Bechinger, Tuning the motility and directionality of self-propelled colloids, Sci. Rep. **7**, 14891 (2017).
[29] C. Shen and H. D. Ou-Yang, The far-from- equilibrium fluctuation of an active Brownian particle in an optical trap, in *Optical Trapping and Optical Micromanipulation XVI*, edited by K. Dholakia and G. C. Spalding, International Society for Optics and Photonics (SPIE, Bellingham, WA, 2019), Vol. 11083, pp. 84–91.
[30] S. C. Takatori, R. De Dier, J. Vermant, and J. F. Brady, Acoustic trapping of active matter, Nat. Commun. **7**, 10694 (2016).
[31] D. Takagi, J. Palacci, A. B. Braunschweig, M. J. Shelley, and J. Zhang, Hydrodynamic capture of microswimmers into sphere-bound orbits, Soft Matter **10**, 1784 (2014).
[32] J. Simmchen, J. Katuri, W. E. Uspal, M. N. Popescu, M. Tasinkevych, and S. Sánchez, Topographical pathways guide chemical microswimmers, Nat. Commun. **7**, 10598 (2016).
[33] See Supplemental Material at http://link.aps.org/supplemental/10.1103/PhysRevLett.129.138002 for details on the theoretical approach and additional calculations.
[34] L. Caprini, F. Cecconi, and U. Marini Bettolo Marconi, Correlated escape of active particles across a potential barrier, J. Chem. Phys. **155**, 234902 (2021).
[35] L. Caprini, U. Marini Bettolo Marconi, A. Puglisi, and A. Vulpiani, Active escape dynamics: The effect of persistence on barrier crossing, J. Chem. Phys. **150**, 024902 (2019).
[36] A. Sharma, R. Wittmann, and J. M. Brader, Escape rate of active particles in the effective equilibrium approach, Phys. Rev. E **95**, 012115 (2017).
[37] E. Woillez, Y. Kafri, and V. Lecomte, Nonlocal stationary probability distributions and escape rates for an active Ornstein–Uhlenbeck particle, J. Stat. Mech. (2020) 063204.
[38] Y. Fily, Self-propelled particle in a nonconvex external potential: Persistent limit in one dimension, J. Chem. Phys. **150**, 174906 (2019).
[39] E. Woillez, Y. Zhao, Y. Kafri, V. Lecomte, and J. Tailleur, Activated Escape of a Self-Propelled Particle from a Metastable State, Phys. Rev. Lett. **122**, 258001 (2019).
[40] L. Zanovello, P. Faccioli, T. Franosch, and M. Caraglio, Optimal navigation strategy of active Brownian particles in target-search problems, J. Chem. Phys. **155**, 084901 (2021).
[41] A. Scacchi and A. Sharma, Mean first passage time of active Brownian particle in one dimension, Mol. Phys. **116**, 460 (2018).
[42] J. Elgeti, R. G. Winkler, and G. Gompper, Physics of microswimmers-single particle motion and collective behavior: A review, Rep. Prog. Phys. **78**, 056601 (2015).
[43] J. Elgeti and G. Gompper, Self-propelled rods near surfaces, Europhys. Lett. **85**, 38002 (2009).
[44] J. Elgeti and G. Gompper, Wall accumulation of self-propelled spheres, Europhys. Lett. **101**, 48003 (2013).
[45] A. Kaiser, H. H. Wensink, and H. Löwen, How to Capture Active Particles, Phys. Rev. Lett. **108**, 268307 (2012).
[46] T. Ostapenko, F. J. Schwarzendahl, T. J. Böddeker, C. T. Kreis, J. Cammann, M. G. Mazza, and O. Bäumchen, Curvature-Guided Motility of Microalgae in Geometric Confinement, Phys. Rev. Lett. **120**, 068002 (2018).
[47] L. Angelani, Confined run-and-tumble swimmers in one dimension, J. Phys. A **50**, 325601 (2017).
[48] J. Elgeti and G. Gompper, Run-and-tumble dynamics of self-propelled particles in confinement, Europhys. Lett. **109**, 58003 (2015).
[49] J. Tailleur and M. Cates, Sedimentation, trapping, and rectification of dilute bacteria, Europhys. Lett. **86**, 60002 (2009).
[50] R. Wittmann and J. M. Brader, Active Brownian particles at interfaces: An effective equilibrium approach, Europhys. Lett. **114**, 68004 (2016).
[51] K. Schaar, A. Zöttl, and H. Stark, Detention Times of Microswimmers Close to Surfaces: Influence of Hydrodynamic Interactions and Noise, Phys. Rev. Lett. **115**, 038101 (2015).
[52] P. Malgaretti and H. Stark, Model microswimmers in channels with varying cross section, J. Chem. Phys. **146**, 174901 (2017).
[53] G. Szamel, Self-propelled particle in an external potential: Existence of an effective temperature, Phys. Rev. E **90**, 012111 (2014).
[54] I. N. Mamede, P. E. Harunari, B. A. N. Akasaki, K. Proesmans, and C. E. Fiore, Obtaining efficient thermal engines from interacting Brownian particles under time-periodic drivings, Phys. Rev. E **105**, 024106 (2022).
[55] J. Lin, K. Li, J. He, J. Ren, and J. Wang, Power statistics of Otto heat engines with the Mpemba effect, Phys. Rev. E **105**, 014104 (2022).
[56] H. C. Berg, *Random Walks in Biology* (Princeton University Press, Princeton, NJ, 2018).